High Resolution Topography along the Lost River Valley, Idaho (USA), April 2019

Simone Bello[1-2] (simone.bello@unich.it), Chelsea Scott[3], J Ramon Arrowsmith[3], Tyler Scott[3]

[1]DiSPUTer - Department of Psychological, Humanistic and Territorial Sciences, University G. d'Annunzio Chieti-Pescara, Italy.
[2]CRUST - InterUniversity Center for 3D Seismotectonics with Territorial applications, Italy
[3]School of Earth and Space Exploration – Arizona State University

Summary

This report accompanies high resolution topography data and orthomosaic imagery acquired during spring 2019 along the Lost River Valley, Idaho. We imaged key areas along the Lost River Fault in Southern Idaho (USA), responsible for the 1983 Borah Peak earthquake (M_w 6.9) both on segments activated and not activated by the earthquake.

In our campaign we acquired ~10,200 photographs using a DJI Phantom 4 Pro and a Phantom 4 Unmanned Aerial Vehicles (UAVs) that flew at ~50-110 meters above ground. In total, we covered ~20 km along the strike of the Lost River Fault at 13 different areas with an average width (fault trace normal) of ~417 m (Figure 1). Point clouds, digital surface models (DSMs), and orthomosaics were generated.

The major reason for acquiring these data was to systematically measure fault vertical separation to produce the most comprehensive throw dataset along the fault activated in the 1983 earthquake as well as in prehistoric earthquakes, providing a database comparable to other earthquakes to better understand coseismic faulting processes, refine scaling laws, and further develop global probabilistic hazard calculations. (*Bello et al., in prep.*) We assigned an identification number to each area according to the identification numbers reported for areas in *Bello et al. (in prep.)*.

OpenTopography

Site Information

Area ID	Area name	Fault	Segment	Area (km^2)	Length along strike (m)	Mean width (m)	Date	Site conditions
1	Hole-in-Rock Creek	LRF	CHS	~0.35	~845	~420	28-apr-19	Variable from sunny to partly cloudy - weak wind.
2	Lime Creek	LRF	CHS	~0.39	~943	~400	28-apr-19	Variable from sunny to partly cloudy - weak wind.
4	Broken Wagon Creek	LPF	LPF	~1.2	~2800	~390	27-apr-19	Sunny - no wind.
6	Dickey Peak	LRF	TSS	~0.16	~740	~210	26-apr-19	Variable from sunny to partly cloudy - moderate wind, cold temperatures.
8	Thousand Springs	LRF	TSS	~3.18	~7721	~500	from 25 to 28-apr-19	Variable from sunny to partly cloudy - weak wind.
9	Southern Thousand Springs	LRF	TSS	~0.13	~570	~210	26-apr-19	Variable from sunny to partly cloudy - moderate wind, cold temperatures.
10	Petes Creek	LRF	MS	~1	~2117	~470	18-apr-19	Sunny - weak or absent wind.
11	Mahogany Gulch	LRF	MS	~0.79	~1710	~430	19-apr-19	Variable from sunny to partly cloudy - weak wind.
12	Jepson Canyon	LRF	PCS	~0.48	~1487	~340	19-apr-19	Variable from sunny to partly cloudy - weak wind.
13	Maddock canyon	LRF	PCS	~0.44	~1020	~470	20-apr-19	Partly cloudy - weak wind.
14	Ramshorn Canyon	LRF	PCS	~0.91	~1300	~750	20-apr-19	Partly cloudy - weak wind.

Table 1 – General site and acquisition information. Key: LRF=Lost River Fault; LPF=Lone Pine Fault; CHS=Challis Segment; TSS=Thousand Springs Segment; MS=Mackay Segment; PCS=Pass Creek Segment.

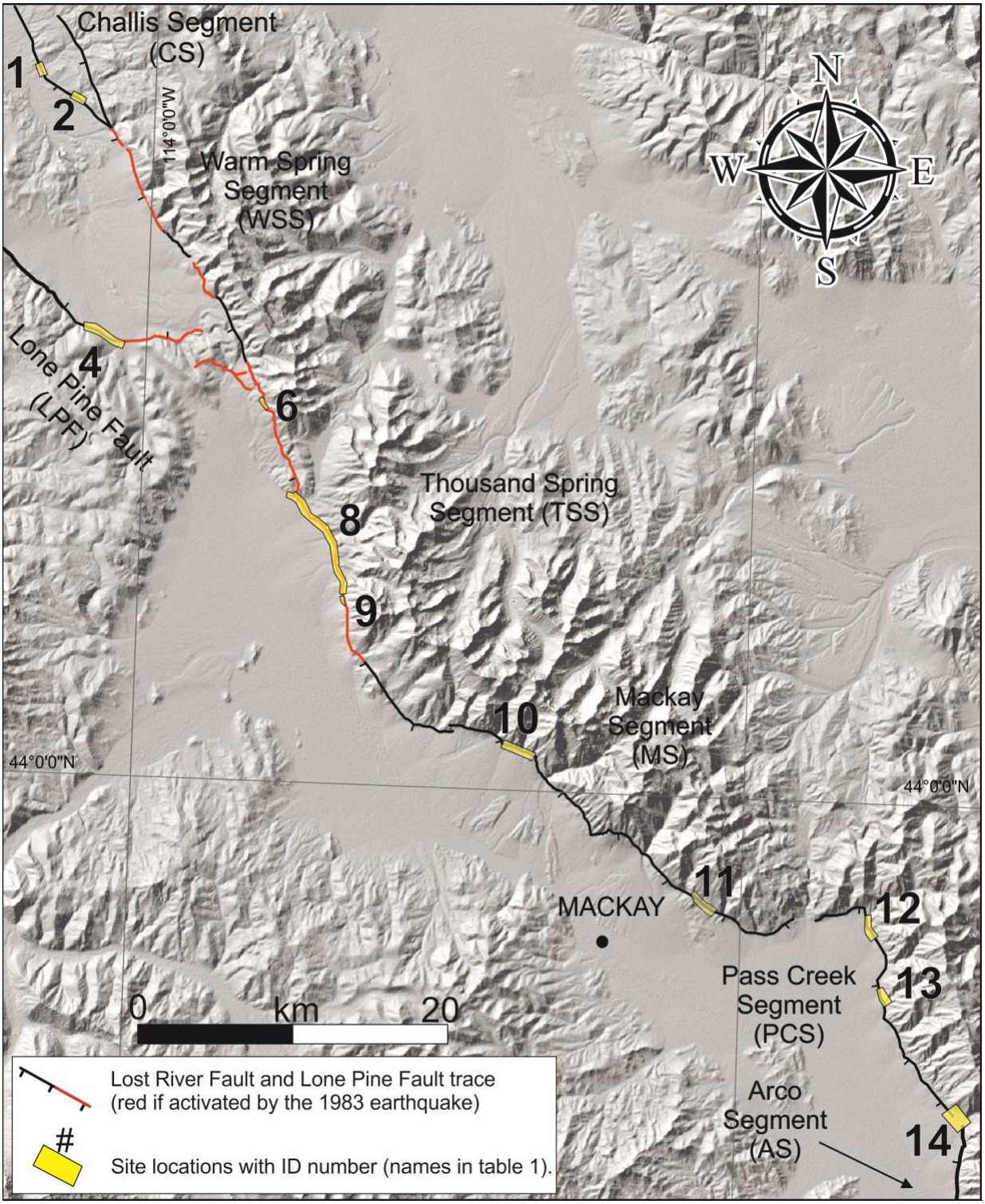

Figure 1 - Location map of areas covered by point clouds, DSMs and orthomosaics (yellow polygons) along the Lost River Fault and Lone Pine Fault.

Equipment used

We used a Phantom 4 Pro UAV and a Phantom 4 UAV to collect the aerial photographs. We generally flew in mission mode, but in places where the topography was particularly irregular and steep, we flew manually (see table 1). We used Pix4DMapper to plan the flight missions. We flew the UAV ~70-120 meters above the take-off point which was often at the base of the tectonic fault scarps we imaged. The camera was for most of the cases pointed 0° from nadir, and, in some cases up to 30° especially for manual flights. We used flight overlaps of ~70% along and perpendicular to the UAV flight track.

GPS and Georeferencing

All images have geolocation information based on onboard GNSS with an accuracy error of approximately ~10m. Along the Thousand Springs Segment and Mackay Segment (areas 8 and 10), we also use measured ground control points (GCP) with a differential GNSS. We place the ~1-m-square black and white vinyl GCP targets on both sides of the fault. Along the Thousand Spring Segment (~4.35 km^2 of imagery), we placed a total of 17 GCP's (~4 GCP/ km^2). We used 12 GCPs on the Mackay Segment (~12 km^2).

We measured GCP locations with a GPS1200 base station and an RX1200 rover with an INTUICOM antenna and a Leica AX1202GG tripod. We had ~4 hours of occupation time for area 8 and ~3 for area 10. We corrected the station locations using the National Geodetic Survey's Online Positioning User Service or (Opus - National Oceanic and Atmospheric Administration, 2018; http://www.ngs.noaa.gov/OPUS/). We reprojected positions into WGS84 UTM zone 12N (EPSG::32612).

See table 2 for a summary of the georeferencing.

Processing

The photographs taken during the fieldwork were manually selected and all those that did not have a high-quality level but were blurred or that were acquired by mistake were eliminated (as for takeoff and landing photos). The selected photographs were subsequently processed with Agisoft Metashape image-based photogrammetric modeling software (versions 1.6.0) to produce dense point clouds, orthomosaics and digital surface models (DSMs) with a resolution between 2 and 30 centimeters per pixel (see Table 2). We processed each of the twelve areas individually. The procedure followed to generate dense point clouds and DSMs is as follows: we uploaded and aligned the photos with "highest" accuracy. For the areas where we used the GCPs, the next step was to load the OPUS-corrected markers. The markers were then manually associated with the corresponding photographs, placing them in the center of each GCP, thus constraining the alignment to fixed points. The accuracy of the measured GCP positions is ~0.02 m in both the horizontal and vertical for area 10. At a few GCPs of area 8, the rover was not able to make the connection with the base station, leading to errors of ~1.2 m and ~2.8 m in the horizontal and vertical coordinates, respectively. The dense cloud was subsequently built with "high" quality. Using the dense clouds as input data, both the DEMs and the orthomosaics were built.

Product parameters

Area ID	1	2	4	6	8	9	10	11	12	13	14
Number of photographs	342	349	1037	314	4495	144	356	1121	577	248	1189
Mean flying altitude (m)	86.7	98.7	116	78.3	102	77	93.5	162	89.2	117	97.5
Ground resolution (m/pix)	0.022	0.025	0.044	0.023	0.076	0.02	0.023	0.041	0.022	0.025	0.024
Reprojection error (pix)	0.50	0.457	0.75	0.567	0.555	0.361	0.861	0.891	0.579	0.441	0.449
Average camera location XY error (m)	4.35	4.23	3.68	3.67	5.79	3.94	4.46	3.60	3.51	5.13	3.02
Average camera location Z error (m)	0.95	0.88	2.16	2.50	10.3	0.91	17.95	3.65	2.35	1.83	2.55
Number of GCPs	-	-	-	-	17	-	12	-	-	-	-
GCP XY RMSE (m)	-	-	-	-	1.16	-	0.22	-	-	-	-
GCP Z RMSE (m)	-	-	-	-	2.8	-	0.096	-	-	-	-
Tie points	236850	201811	424638	223451	3024439	117137	753743	565957	603138	220572	1305679
Dense cloud total points	2.33E+08	1.92E+08	1.99E+08	1.28E+08	1.33E+09	9.09E+07	4.46E+08	1.78E+08	3.10E+08	1.30E+08	5.06E+08
Point density (pts/m2)	539	413	127	604	9.32	606	469	149	502	397	425
DSM resolution (m/pix)	0.043	0.049	0.088	0.041	0.033	0.04	0.046	0.082	0.045	0.05	0.048
Orthomosaic resolution (m/pix)	0.022	0.025	0.044	0.02	0.028	0.02	0.023	0.041	0.024	0.066	0.026

Table 2 – Resolution, accuracy and other descriptive parameters of the surveys and resulting of products.

Personnel and roles:

PI: S. Bello, C. Scott, R. Arrowsmith
Collector: T. Scott
Funder: S. Bello, C. Scott, R. Arrowsmith

Funding:

We acknowledge funding from School of Advanced Studies G. d'Annunzio at 'Gabriele d'Annunzio' University of Chieti-Pescara (Italy) to the "Earthquake and Environmental Hazards" Ph.D. Course, the National Science Foundation Postdoctoral Fellowship 1625221 to Chelsea Scott, the School of Earth & Space Exploration at Arizona State University, and NASA ROSES funding from the Jet Propulsion Laboratory to Arizona State University.